Supplementary Information

Imine Bond-Directed Assembly of Polyoxometalate-Based Metal–Organic Frameworks

Xiang Yu[+], Xinyu Xu[+], Lei Gao, Rengan Luo, Yi-Fan Liu, Yu-Hao Gu, Shuai Yuan*

State Key Laboratory of Coordination Chemistry, School of Chemistry and Chemical Engineering, Nanjing University, Nanjing 210023, China

[+]These authors contributed equally to this work.

Materials and methods

All reagents were of reagent-grade, obtained from commercial sources, and used without further purification. Single-crystal X-ray diffraction intensity data for Zn-POMOF, Co-POMOF, and Fe(III)-POMOF were collected on a Bruker D8 Venture diffractometer. ^{1}H NMR data were recorded on a Bruker Avance III 400 NMR spectrometer. FT-IR spectra were recorded on a Vector 27 Bruker Spectrophotometer by transmission through KBr pellets containing ground crystals in the range 4000-400 cm^{-1}. TGA data were obtained on a TGA 4000 thermal analysis system at a heating rate of 5 °C min^{-1} under an air atmosphere. Powder X-ray diffraction (PXRD) patterns were collected at room temperature at a scan speed of 0.1 s/step on a Bruker Advance D8 (40 kV, 40 mA) diffractometer equipped with Cu radiation. Simulated PXRD patterns were generated from single-crystal data using Mercury 3.0. The morphology and elemental mapping of the samples were characterized by transmission electron microscopy (TEM, JEOL JEM-2800). Metal content was analyzed via inductively coupled plasma optical emission spectroscopy (ICP-OES) using the Jarrell-Ash 1100 + 2000 instrument. The morphology and elemental mapping of samples were characterized by field emission scanning electron microscopy (SEM, Hitachi Regulus SU8230). X-ray photoelectron spectroscopy (XPS) measurements were carried out at a Thermo Fisher Scientific EscaLab 250 Xi (Al Kα radiation, *hv* = 1486.6 eV) equipped with an electron flood gun. XPS data were analyzed using Thermo Fisher Scientific Advantage Data System software and all spectra were referenced to the C 1s peak (284.8 eV). Single-crystal X-ray diffraction intensity data for POM-COOH, Zn-POMOF, Co-POMOF, and Fe(III)-POMOF were collected on a Bruker D8 Venture diffractometer fitted with a PHOTON-100 CMOS detector, monochromatized microfocus Mo Kα radiation (λ= 0.71073 Å), and a nitrogen flow controlled by a KRYOFLEX II low-temperature attachment operating at 193 K. Raw data collection and reduction was controlled using APEX3 software. The structures were solved by direct methods and refined by full-matrix squares least-squares on F2 using the SHELXTL software package.

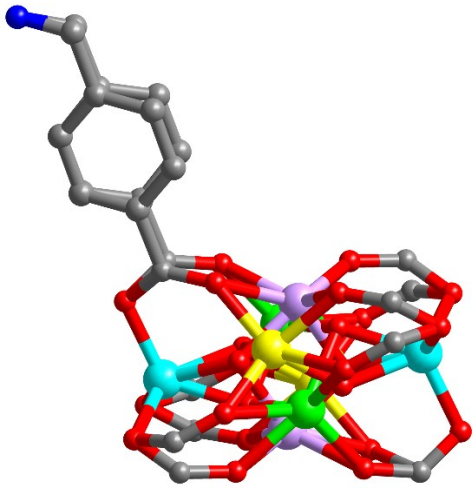

Fig. S1 The single-crystal structure of the $Zn_4(Zn_4(OH)_2(COO)_6(H_2O)_6)$ clusters in Zn-POMOF with three-fold disorders. Zn-POMOF and Co-POMOF are isostructural, consisting of $Zn_4(OH)_2(COO)_6(H_2O)_6$ and $Co_4(OH)_2(COO)_6(H_2O)_6$ clusters, which exhibit identical coordination environments. However, the Zn_4 clusters exhibit disorder, while the Co_4 clusters are ordered in the refined crystal structure.

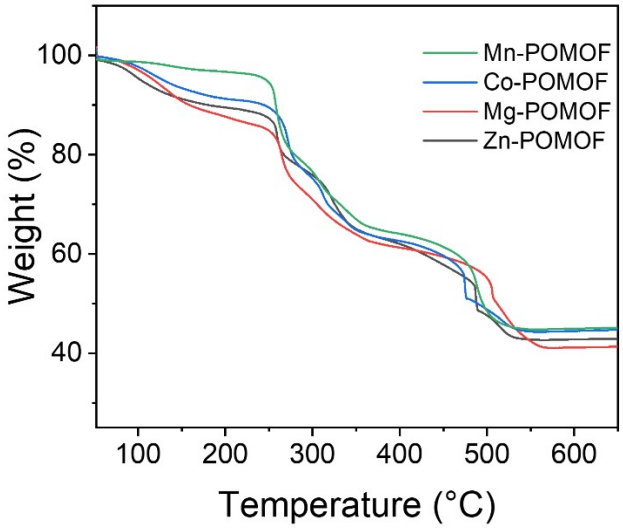

Fig. S2. Thermogravimetric analysis (TGA) of M(II)-POMOFs (M = Zn, Co, Mn, Mg).

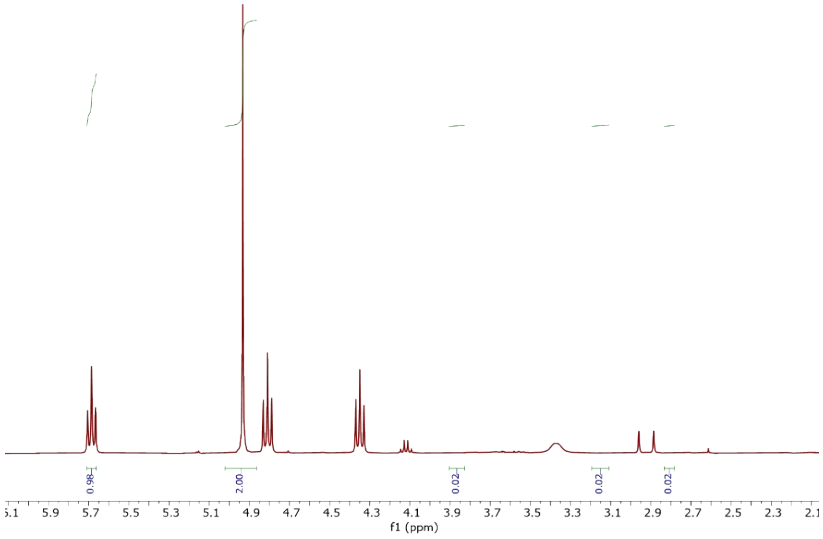

Fig. S3 The yields of the cyclic carbonates were calculated by ^{1}H NMR of the Fe(III)-POMOF using CH_2Br_2 as an internal standard.[1, 2]

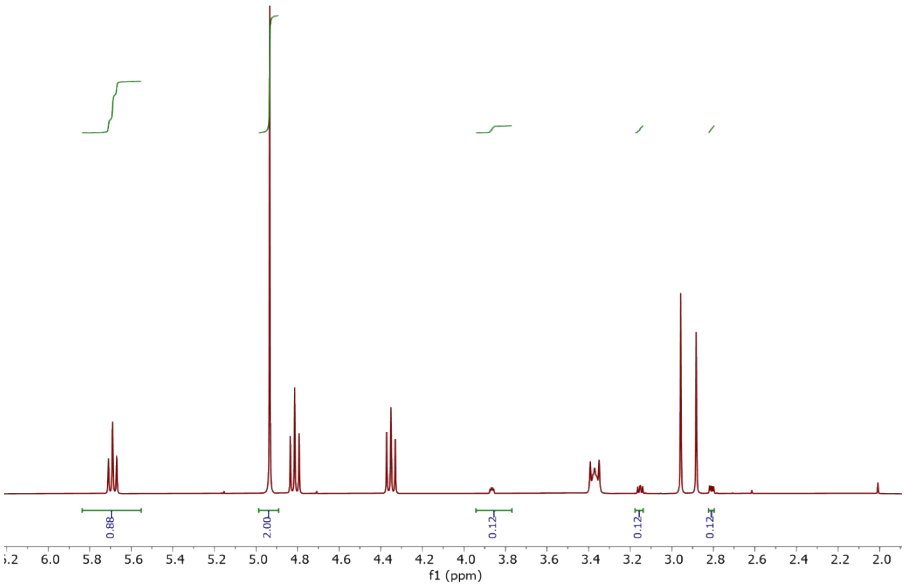

Fig. S4 The yields of the cyclic carbonates were calculated by ^{1}H NMR of Zn-POMOF using CH_2Br_2 as an internal standard.

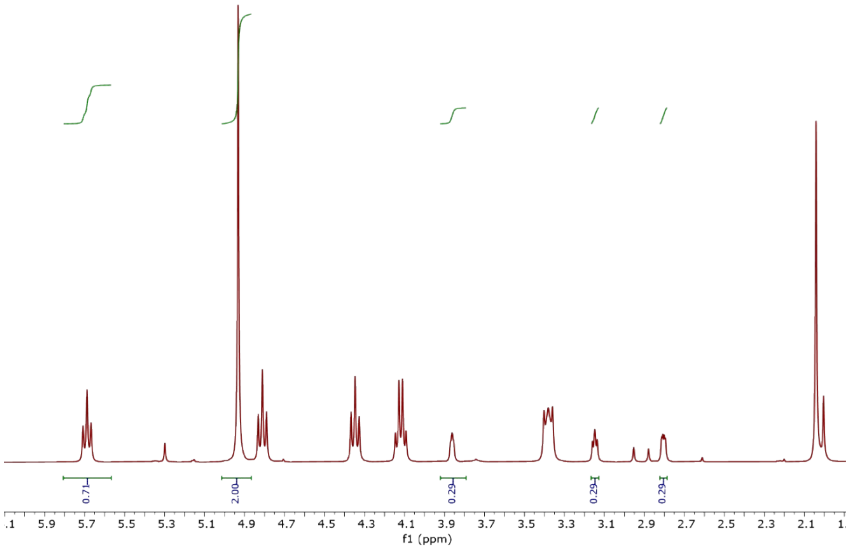

Fig. S5 The yields of the cyclic carbonates were calculated by ^{1}H NMR of Co-POMOF using CH_2Br_2 as an internal standard.

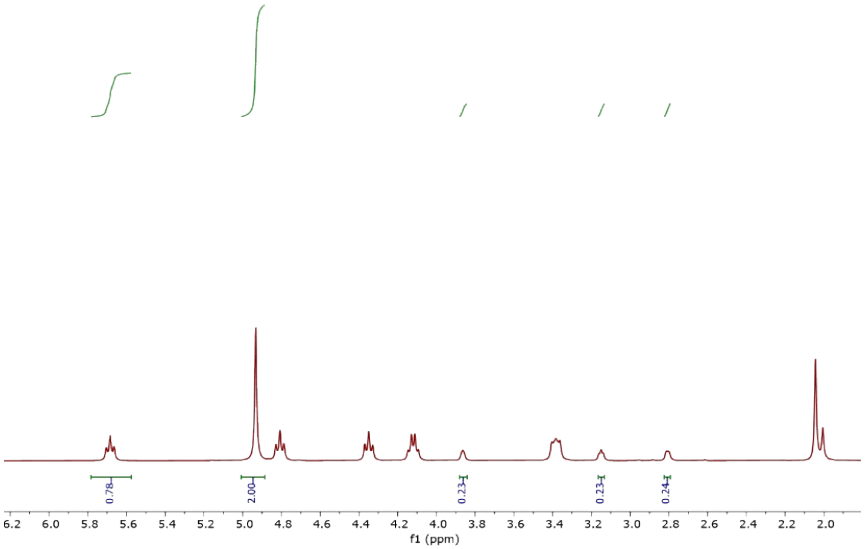

Fig. S6 The yields of the cyclic carbonates were calculated by ^{1}H NMR of the Mn-POMOF using CH_2Br_2 as an internal standard.

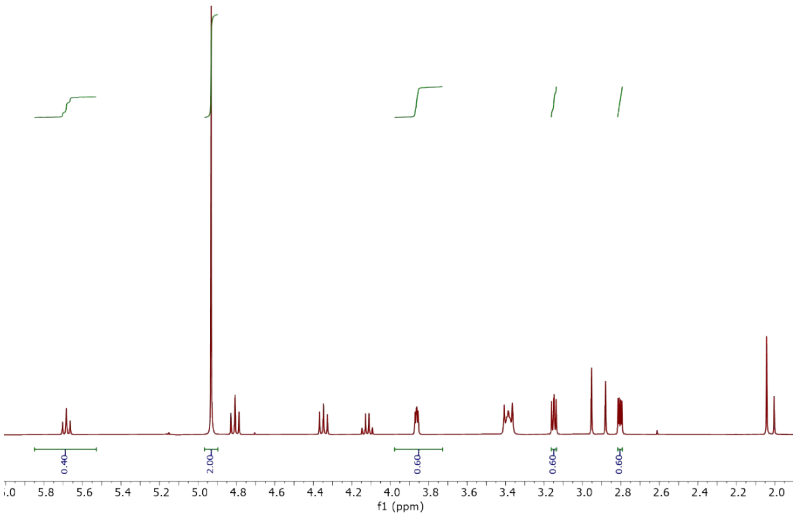

Fig. S7 The yields of the cyclic carbonates were calculated by ^{1}H NMR of the Mg-POMOF using CH_2Br_2 as an internal standard.

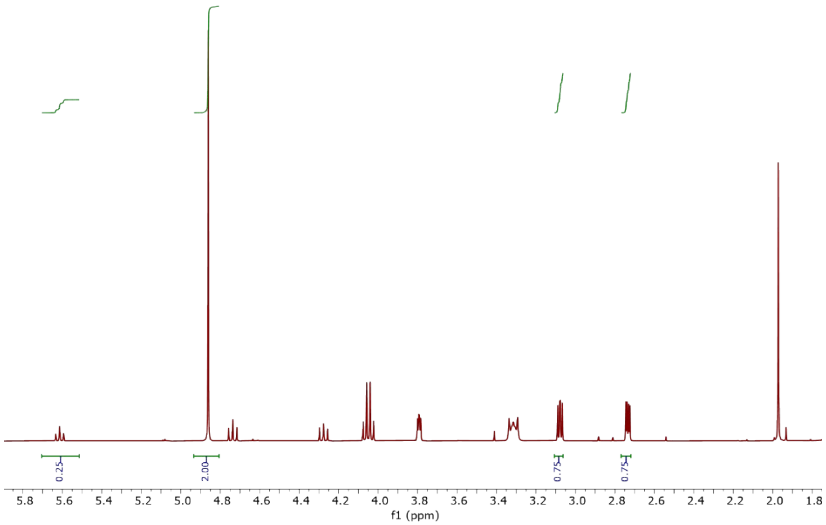

Fig. S8 The yields of the cyclic carbonates were calculated by ^{1}H NMR of a mixture of $FeCl_3$ and POM-COOH using CH_2Br_2 as an internal standard.

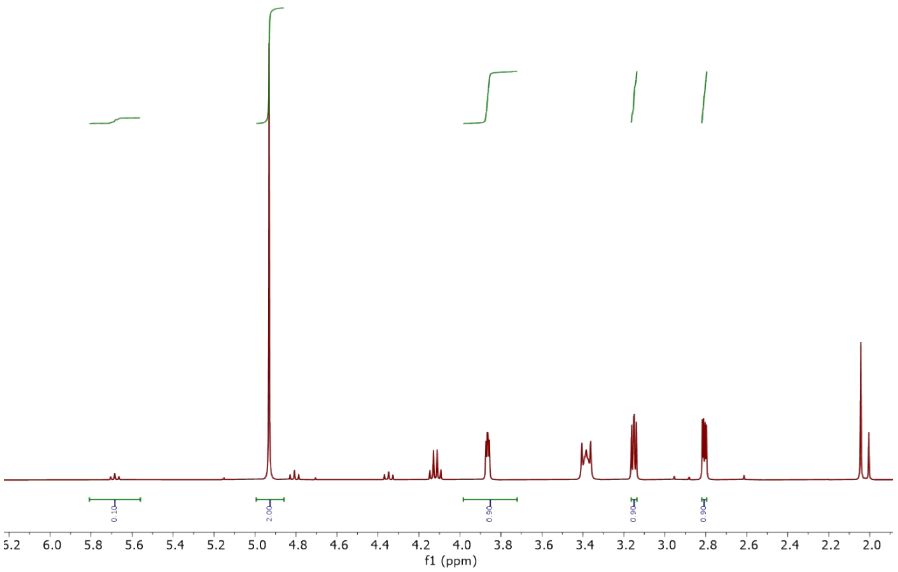

Fig. S9 The yields of the cyclic carbonates were calculated by ^{1}H NMR of POM-COOH using CH_2Br_2 as an internal standard.

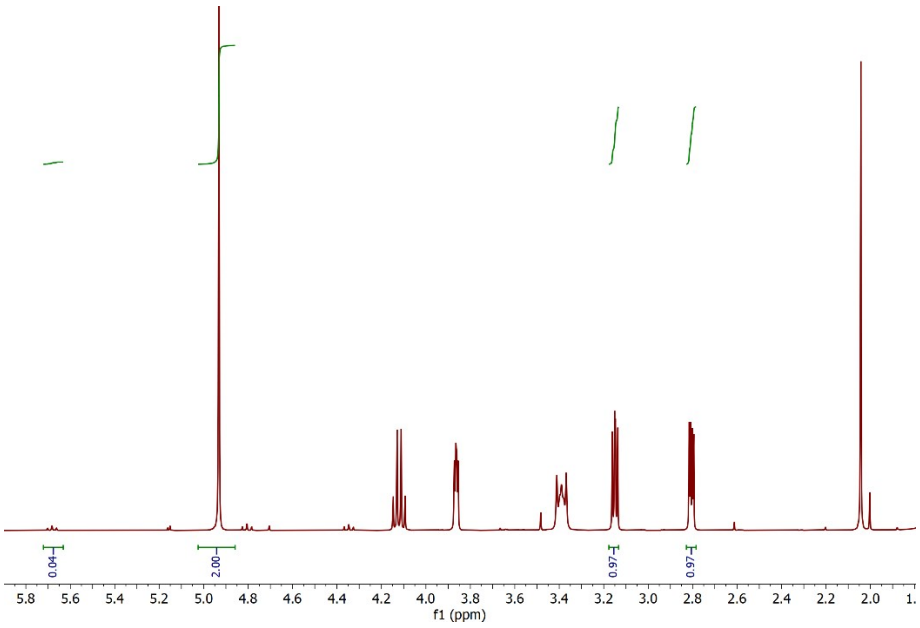

Fig. S10 The yields of the cyclic carbonates were calculated by ^{1}H NMR of $FeCl_3$ using CH_2Br_2 as an internal standard.

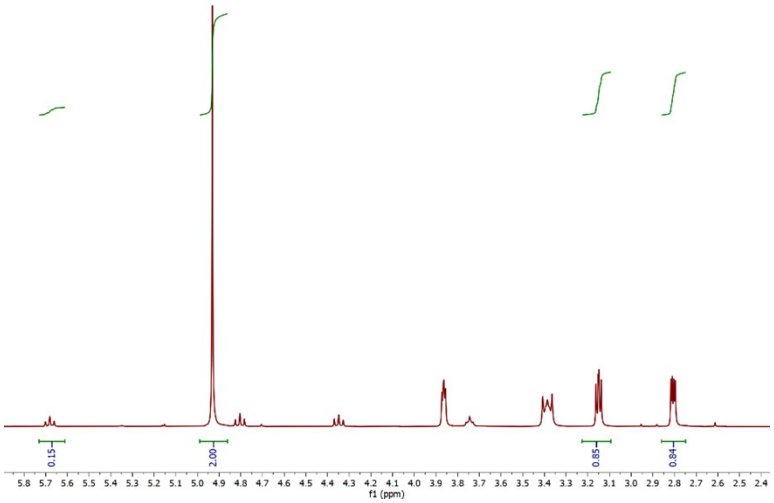

Fig. S11 The yields of the cyclic carbonates were calculated by ^{1}H NMR of PCN-250 using CH_2Br_2 as an internal standard.

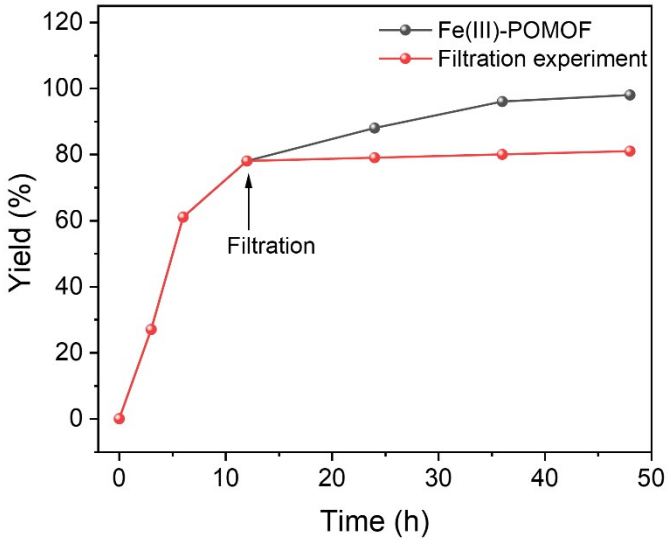

Fig. S12 Hot filtration of the reaction system was performed after 12 h catalytic reaction, then leaving the filtrate for subsequent reaction for 36 h.

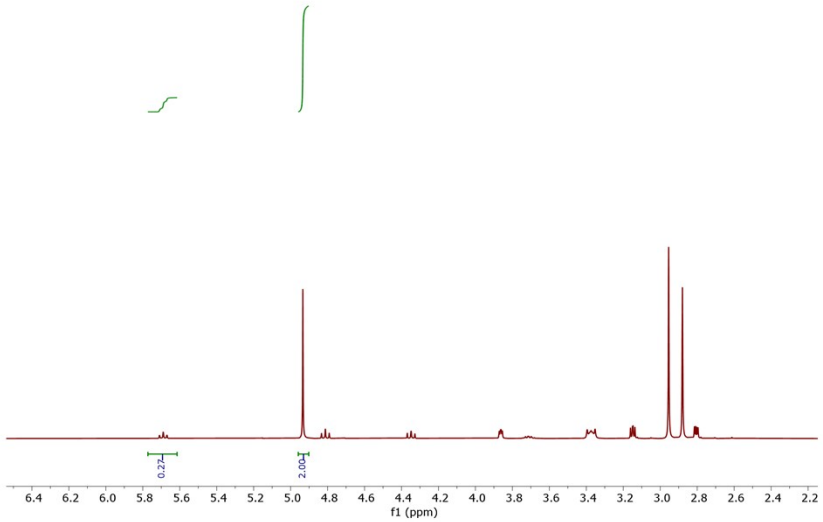

Fig. S13 The yields of the cyclic carbonates for reaction 3 h were calculated by ^{1}H NMR of Fe(III)-POMOF using CH_2Br_2 as an internal standard.

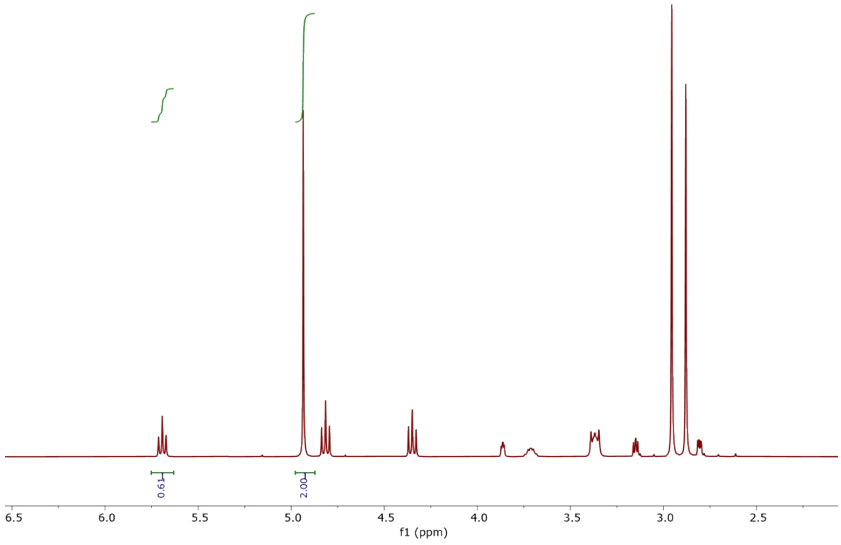

Fig. S14 The yields of the cyclic carbonates for reaction 6 h were calculated by ^{1}H NMR of Fe(III)-POMOF using CH_2Br_2 as an internal standard.

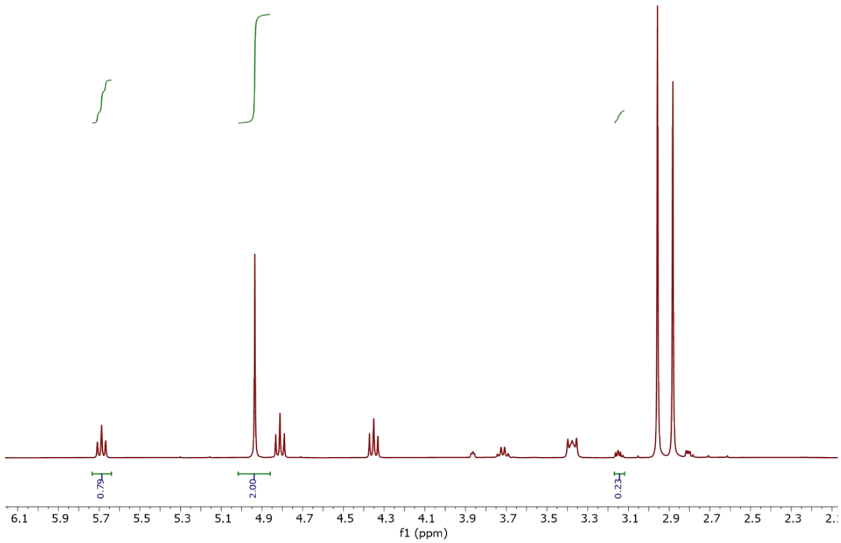

Fig. S15 The yields of the cyclic carbonates for reaction 12 h were calculated by ^{1}H NMR of Fe(III)-POMOF using CH_2Br_2 as an internal standard.

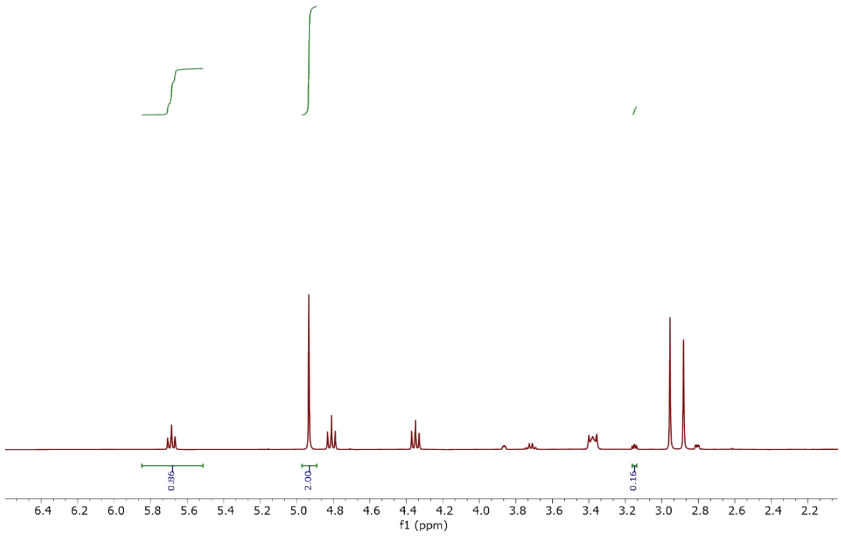

Fig. S16 The yields of the cyclic carbonates for reaction 24 h were calculated by ^{1}H NMR of Fe(III)-POMOF using CH_2Br_2 as an internal standard.

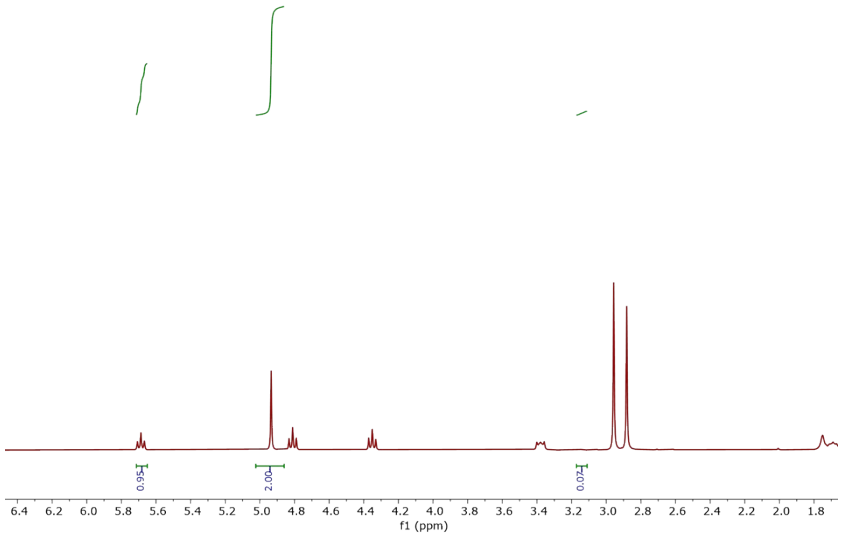

Fig. S17 The yields of the cyclic carbonates for reaction 36 h were calculated by ^{1}H NMR of Fe(III)-POMOF using CH_2Br_2 as an internal standard.

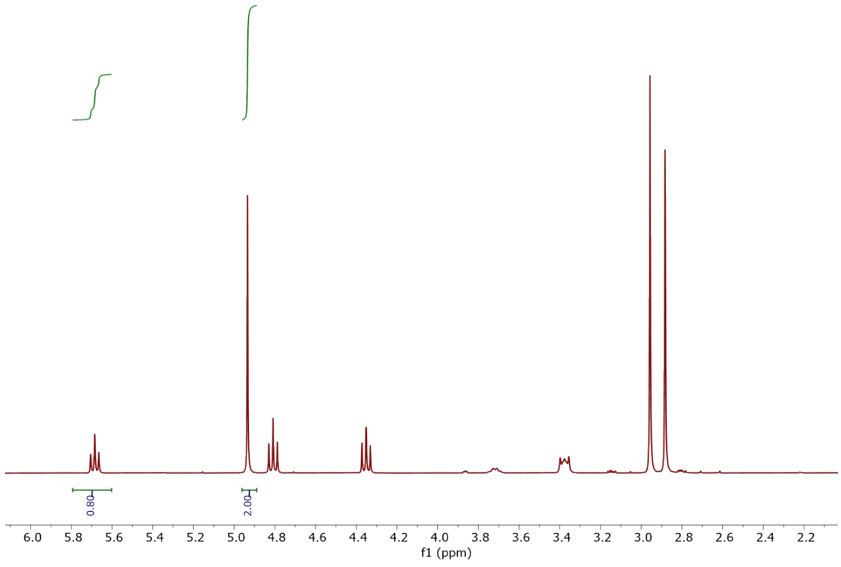

Fig. S18 The yields of the cyclic carbonates after hot filtration were calculated by ^{1}H NMR of Fe(III)-POMOF using CH_2Br_2 as an internal standard.

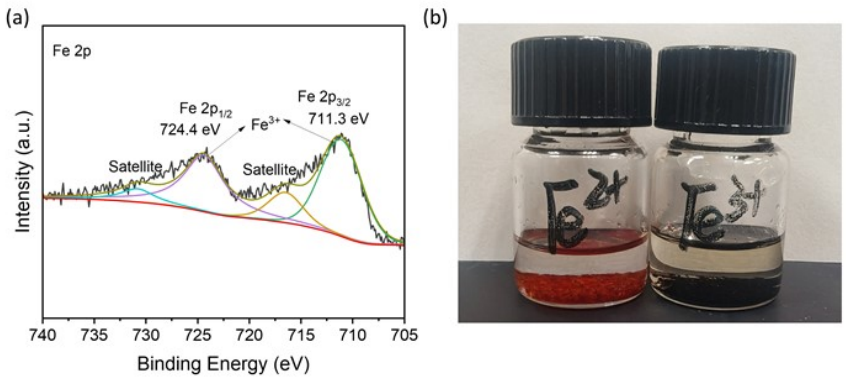

Fig. S19 XPS Fe 2p spectra of Fe(III)-POMOF (a) and the color change of Fe-POMOF (b).

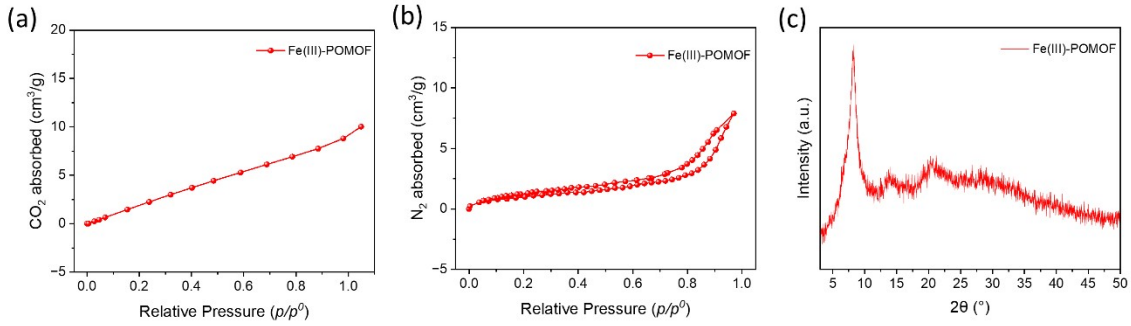

Fig. S20 (a) CO_2 adsorption isotherm of Fe(III)-POMOF at 298K. (b) N_2 adsorption-desorption isotherms of Fe(III)-POMOF at 77 K. (c) PXRD patterns of Fe(III)-POMOF after gas adsorption measurements.

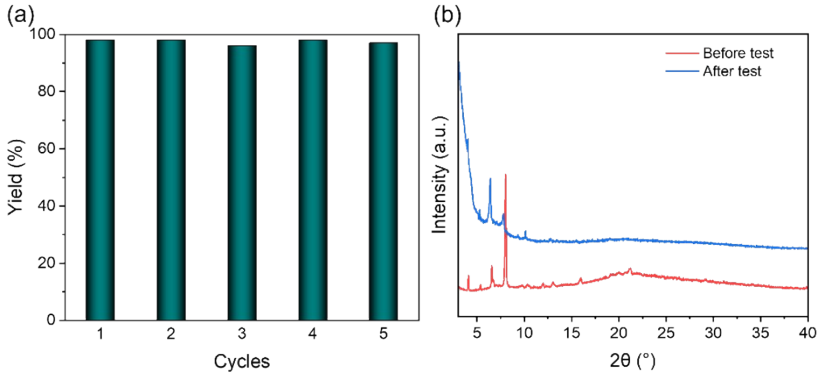

Fig. S21 (a) Cycling experiments with Fe(III)-POMOF and (b) PXRD before and after catalysis.

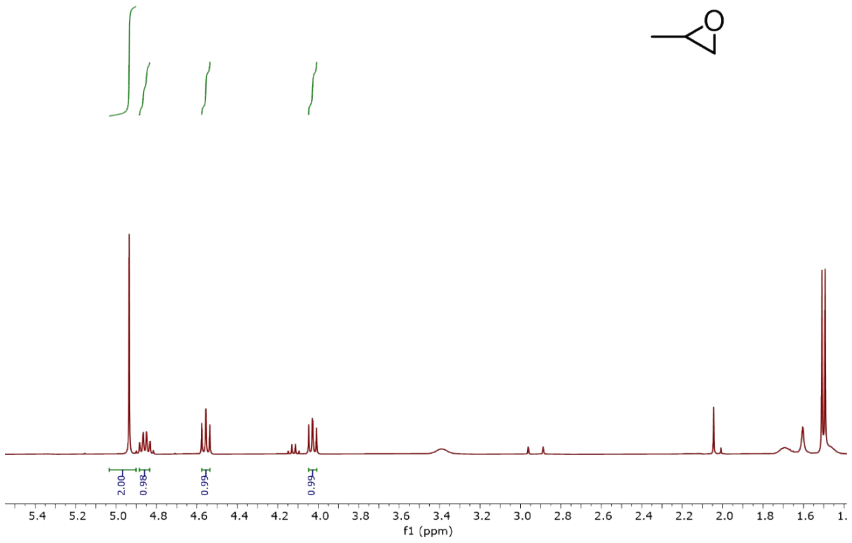

Fig. S22 The yields of the cyclic carbonates were calculated by ^{1}H NMR of propylene oxide using CH_2Br_2 as an internal standard.

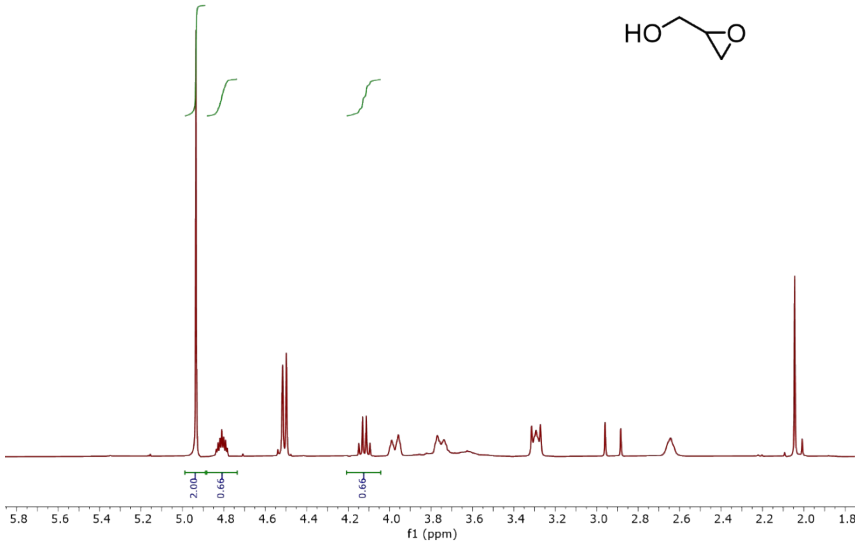

Fig. S23 The yields of the cyclic carbonates were calculated by ^{1}H NMR of epichlorohydrin using CH_2Br_2 as an internal standard.

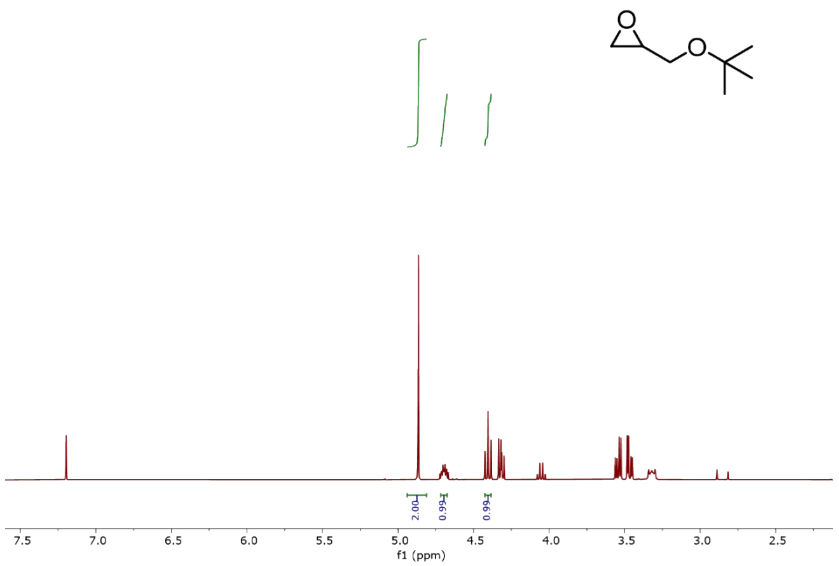

Fig. S24 The yields of the cyclic carbonates were calculated by ^{1}H NMR of 2-(tert-butoxymethyl)oxirane using CH_2Br_2 as an internal standard.

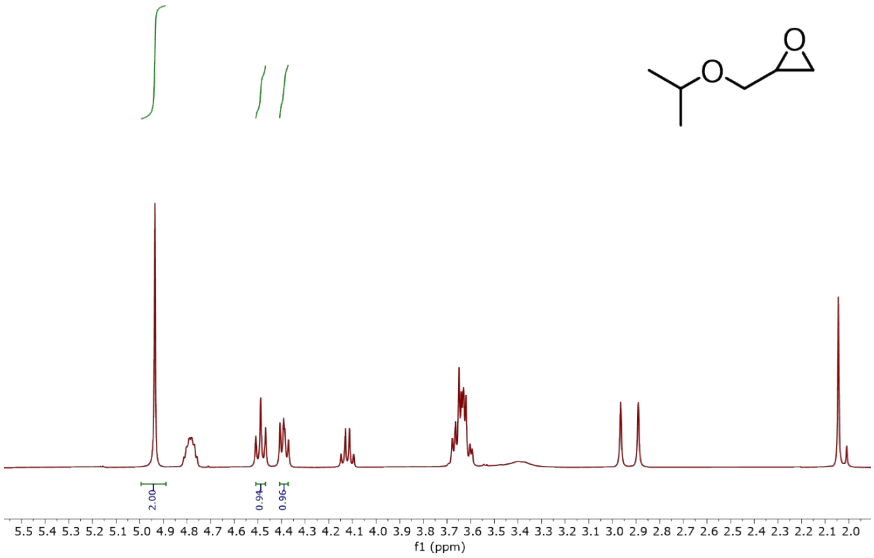

Fig. S25 The yields of the cyclic carbonates were calculated by ^{1}H NMR of 2-(isopropoxy ethyl)oxirane using CH_2Br_2 as an internal standard.

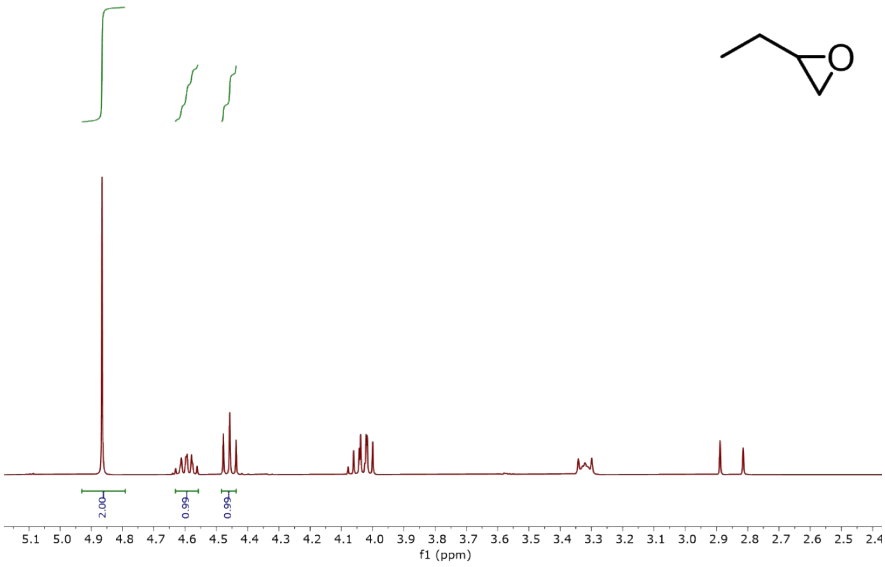

Fig. S26 The yields of the cyclic carbonates were calculated by ^{1}H NMR of 2-methyl oxirane using CH_2Br_2 as an internal standard.

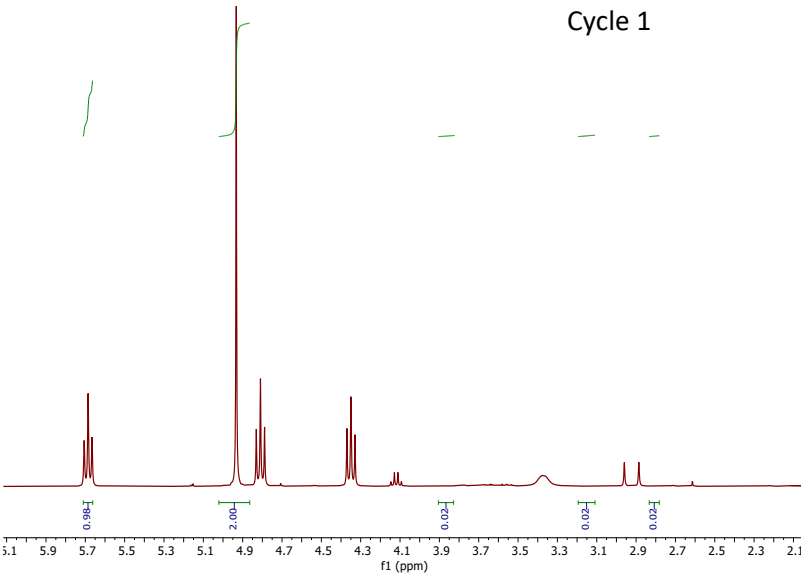

Fig. S27 The cyclic carbonate yields of 1st cycle were calculated by ^{1}H NMR using CH_2Br_2 as an internal standard.

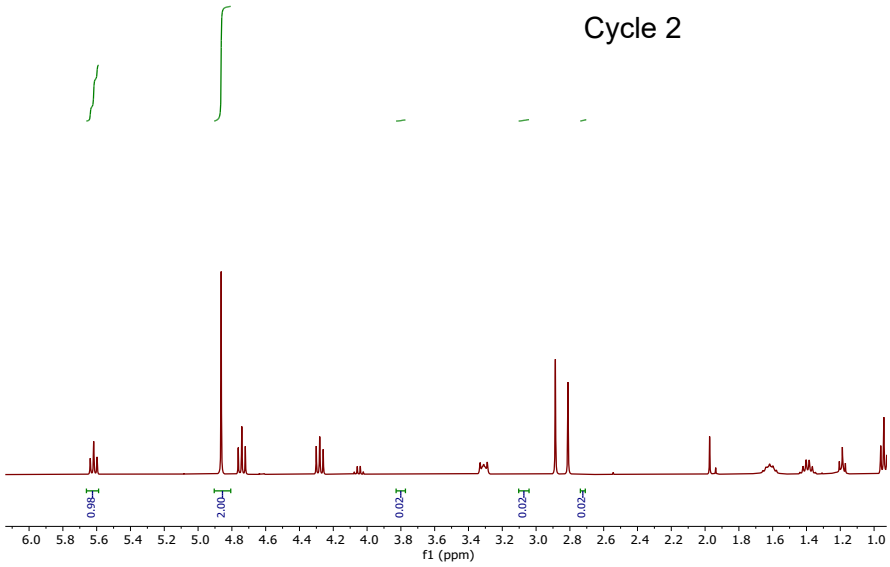

Fig. S28 The cyclic carbonate yields of 2nd cycle were calculated by ^{1}H NMR using CH_2Br_2 as an internal standard.

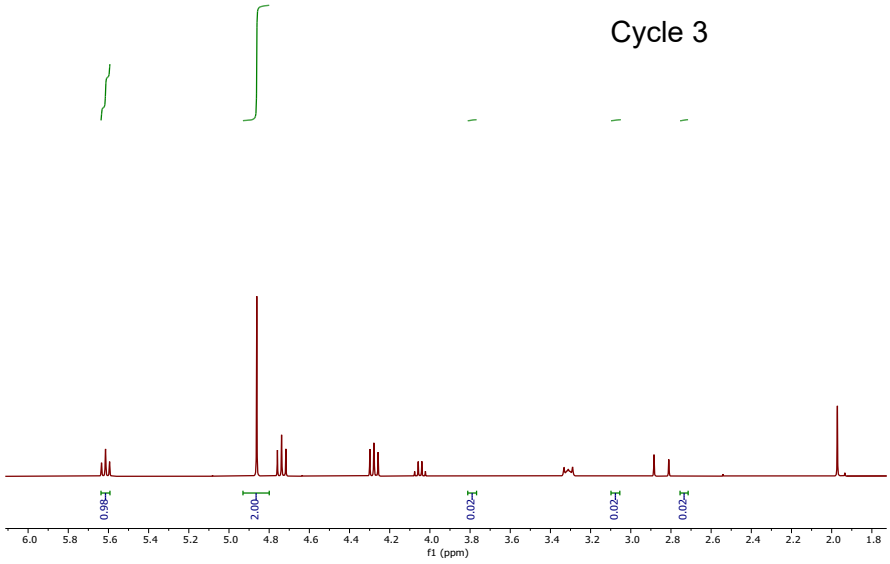

Fig. S29 The cyclic carbonate yields of 3rd cycle were calculated by ^{1}H NMR using CH_2Br_2 as an internal standard.

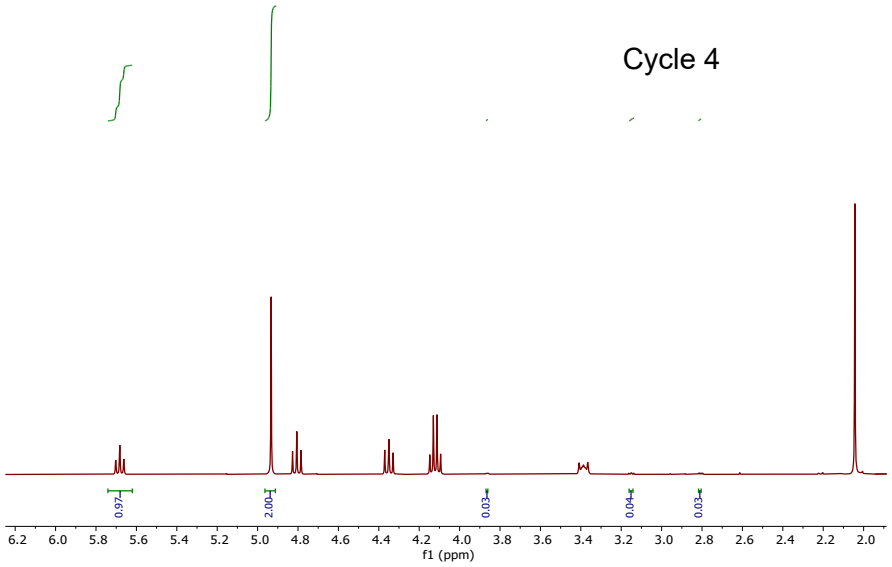

Fig. S30 The cyclic carbonate yields of the 4th cycle were calculated by ^{1}H NMR using CH_2Br_2 as an internal standard.

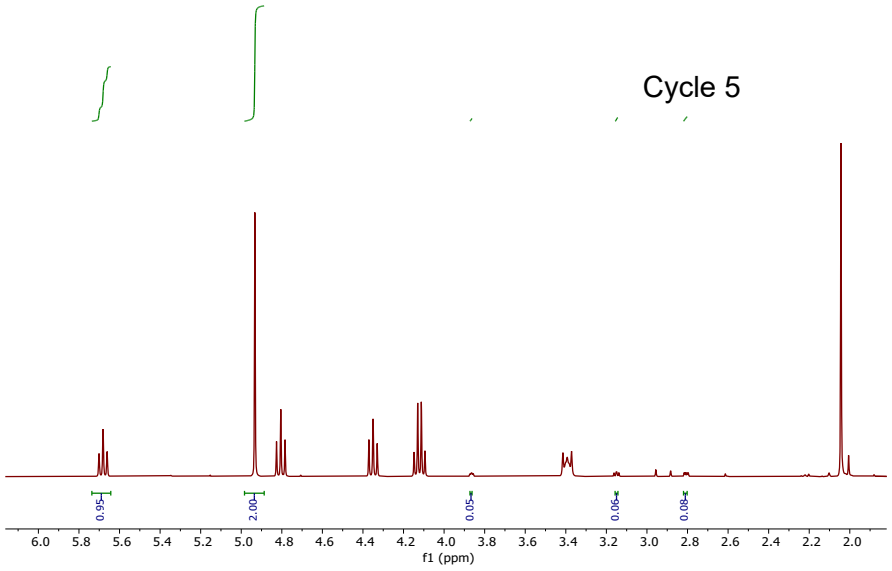

Fig. S31 The cyclic carbonate yields of the 5th cycle were calculated by ^{1}H NMR using CH_2Br_2 as an internal standard.

Table S1. The Crystallographic data for POM-COOH and M-POMOFs.

Name	POM-COOH	Zn-POMOF	Co-POMOF	Fe(III)-POMOF
CCDC	2381572	2381573	2381574	2381575
Empirical formula	$C_{95}H_{186}MnMo_6N_6O_{31.5}S_{3.5}$	$C_{36}H_{33}Mn_{1.5}Mo_9N_3O_{43}Zn_2$	$C_{145}H_{129}Co_8Mn_6Mo_{36}N_{12}O_{180}$	$C_{36}H_{33}Fe_2Mn_{1.5}Mo_9N_3O_{43}$
Formula weight	2659.28	2272.26	9174.51	2253.22
Temperature/K	193.00	193.00	153.00	173.00k
Crystal system	triclinic	trigonal	monoclinic	trigonal
Space group	P-1	R-3m	$P2_1/n$	R-3m
a/Å	16.5890(17)	45.047(2)	18.5098(16)	45.266(18)
b/Å	17.1075(18)	45.047	44.611(3)	45.266(18)
c/Å	22.616(2)	18.7659(10)	26.993(2)	18.250(7)
α/°	90.450(4)	90	90	90
β/°	106.263(4)	90	102.893(4)	90
γ/°	95.652(4)	120	90	120
Volume/Å^3	6127.2(11)	32979(4)	21727(3)	32385(28)
Z	2	6	1	6
ρ_{calc}g/cm^3	1.441	0.686	0.701	0.693
μ/mm^{-1}	4.588	0.821	4.248	0.749
F(000)	2766.0	6537.0	4401.0	6489.0
Crystal size/mm^3	0.23 × 0.22 × 0.2	0.23 × 0.14 × 0.1	0.2 × 0.15 × 0.1	0.3 × 0.25 × 0.2
Radiation	GaKα (λ = 1.34139)	MoKα (λ = 0.71073)	GaKα (λ = 1.34138)	MoKα (λ = 0.71073)
2Θ range for data collection/°	3.544 to 105.964	3.512 to 50.114	3.392 to 106.758	3.54 to 44.996
Index ranges	-19 ≤ h ≤ 19, -20 ≤ k ≤ 20, -26 ≤ l ≤ 26	-53 ≤ h ≤ 53, -53 ≤ k ≤ 53, -22 ≤ l ≤ 22	-22 ≤ h ≤ 21, -52 ≤ k ≤ 53, -25 ≤ l ≤ 32	-46 ≤ h ≤ 48, -48 ≤ k ≤ 48, -19 ≤ l ≤ 19
Reflections collected	62217	84385	165304	57376
Independent reflections	21332 [R_{int} = 0.0488, R_{sigma} = 0.0490]	6767 [Rint = 0.0832, Rsigma = 0.0413]	38636 [R_{int} = 0.0867, R_{sigma} = 0.1005]	4934 [R_{int} = 0.1548, R_{sigma} = 0.0823]
Goodness-of-fit on F^2	1.071	1.020	0.902	0.818
Final R indexes [I>=2σ (I)]	R_1 = 0.0833, wR_2 = 0.2149	R_1 = 0.0894, wR_2 = 0.2815	R_1 = 0.0784, wR_2 = 0.2495	R_1 = 0.0903, wR_2 = 0.2849
Final R indexes [all data]	R_1 = 0.0883, wR_2 = 0.2173	R_1 = 0.1454, wR_2 = 0.3582	R_1 = 0.1491, wR_2 = 0.2988	R_1 = 0.1849, wR_2 = 0.3151

$R_1 = \Sigma||Fo|-|Fc||/\Sigma|Fo|$. $wR_2 = |\Sigma w(|Fo|^2\ |Fc|^2)|/\Sigma|w(Fo^2)^2|^{1/2}$

References

1. L. Zhang, S. Yuan, W. Fan, J. Pang, F. Li, B. Guo, P. Zhang, D. Sun and H.-C. Zhou, *ACS Appl. Mater. Interfaces*, 2019, **11**, 22390-22397.
2. H.-Q. Yin, M.-Y. Cui, H. Wang, Y.-Z. Peng, J. Chen, T.-B. Lu and Z.-M. Zhang, *Inorg. Chem.*, 2023, **62**, 13722-13730.